Article

Impact of Pressure and Temperature on Foam Behavior for Enhanced Underbalanced Drilling Operations

Ahmed Gowida, Salaheldin Elkatatny,* Ahmed Farid Ibrahim, and Muhammad Shahzad Kamal

Cite This: *ACS Omega* 2024, 9, 1042−1055

Read Online

ACCESS | Metrics & More | Article Recommendations

ABSTRACT: Foam, a versatile underbalanced drilling fluid, shows potential for improving the drilling efficiency and reducing formation damage. However, the existing literature lacks insight into foam behavior under high-pH drilling conditions. This study introduces a novel approach using synthesized seawater, replacing the conventional use of freshwater on-site for the foaming system's liquid base. This approach is in line with sustainability objectives and offers novel perspectives on foam stability under high-pH conditions. Experiments, conducted with a high-pressure, high-temperature (HPHT) foam analyzer, investigate how pressure and temperature affect foam properties. The biodegradable foaming agent ammonium alcohol ether sulfate (AAES) is employed. Results demonstrate that the pressure significantly impacts foam stability. Increasing pressure enhances stability, reducing decay rates and promoting uniform bubble sizes, especially at lower temperatures. This highlights foam's capacity to withstand high-pressure conditions. Conversely, the temperature plays a substantial role in foam decay, particularly at elevated temperatures (75 and 90 °C). Decreased liquid viscosity accelerates the liquid drainage and foam decay. While pressure mainly influences the AAES foam stability at temperatures up to 50 °C, temperature becomes the dominant factor at higher temperatures. Temperature's impact on foamability is minimal under constant pressure, maintaining consistent gas volume for maximum foam height. However, foam stability is sensitive to temperature variations, with increasing temperature leading to a more significant bubble size increase gradient. These findings stress the importance of considering temperature effects in foam drilling, particularly in deep and high-temperature environments. AAES foam exhibits stability at lower temperatures, making it suitable for surface and intermediate drilling. Understanding temperature-induced changes in foam structure and bubble size is essential for optimizing performance in high-temperature and deep drilling scenarios.
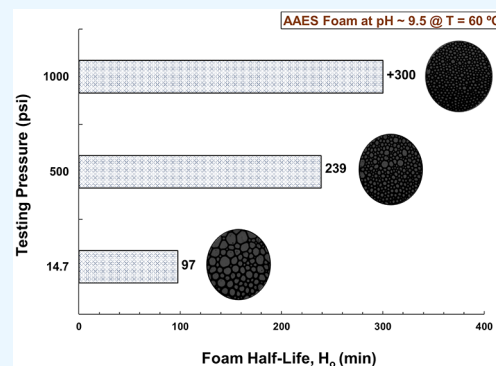
1. INTRODUCTION

Foam has emerged as a versatile fluid for underbalanced drilling applications.[1] Its unique properties and characteristics make it particularly useful for enhancing underbalanced drilling operations. Foam comprises a two-phase system wherein gas bubbles are dispersed within a liquid phase, often water or oil.[2] It enhances drilling efficiency and hole stability by reducing the influx of formation fluids, thereby mitigating the risk of wellbore collapse.[3] Its low density and high viscosity enable efficient transport of drilled cuttings to the surface, leading to improved hole cleaning.[1]

Foam Stability. Foam stability is a crucial characteristic in foaming systems, describing how the foam volume or height changes over time after its formation. To quantify foam stability, scientists assess the foam bubbles' half-life (H_o), representing the time it takes for the foam volume to decrease to half of its initial value due to foam decay. Determining H_o involves calculating the relative foam volume (RFV), which indicates the percentage of remaining foam volume compared to the maximum foam volume after foaming has ceased. The RFV is obtained using the following equation:

$$\text{RFV}(t) = \frac{V_t(\text{foam})}{V_{\text{Initial}}(\text{foam})} \times 100\%$$

(1)

where V represents the foam volume observed in a transparent cell; the subscript t refers to the measured foam volume at a specific time; and V_{Initial} denotes the initial foam volume right after the bubbling stops.[4] By continuously monitoring the RFV values over time, one can estimate H_o by calculating the duration required for the foam volume to decrease to 50% of its initial value, which is represented by RFV equal to 0.5.[5]
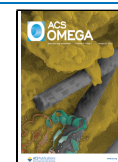
In the realm of foam applications, the principal factor influencing surfactant selection is commonly acknowledged to be foam stability.[6] Upon the generation of foam, there exists the

potential for liquid drainage driven by gravitational forces, leading to foam destabilization.[4] It is noteworthy that higher foam viscosity does not consistently yield enhanced foam stability; its impact can vary, depending on the application. In some scenarios, increased viscosity can improve stability through film thinning, while in others, it can impede stability.[7]

Numerous factors impact the stability and formation of foam, including surfactant adsorption at the liquid/gas interface, pressure, temperature, and salinity.[8] For instance, higher pressure has a favorable impact on foam stability, as evidenced by a study indicating that increasing pressure leads to a prolongation of foam half-life.[9] Additionally, another investigation examined the characteristics of foam using Armovis as a surfactant, comparing conditions at ambient pressure and 1000 psi (6894.76 kPa).[10] This analysis revealed that an elevated pressure resulted in smaller bubble radii and denser foam. Conversely, elevated temperatures tend to diminish foam stability due to surfactant degradation.[11]

The current literature presents a range of conflicting findings pertaining to the impact of salts on foam characterization. For instance, Guo et al.[12] conducted an investigation into the influence of salt concentration on foam stability under ambient conditions. Their findings indicated a notable increase in foam half-life with an escalating NaCl concentration, attributed to a reduced drainage rate and reinforced bubble film strength. They claimed that the enhancement in foam stability arose from the heightened electrostatic forces between micelles, consequently resulting in increased viscosity.

Furthermore, Majeed et al.[13] conducted multiple experiments to investigate the effect of NaCl concentration on foam properties, including foamability and stability under ambient conditions. Interestingly, their results unveiled that the influence of salt on foam could be stabilizing or destabilizing contingent on the surfactant concentration. With the addition of 1 M NaCl to a 0.025 wt % surfactant solution, foam decreased 7-fold, but when surfactant concentration was elevated to 0.25 wt %, the foam's half-life improved 6-fold with the inclusion of 1 M NaCl.

Moreover, AlYousef et al.[14] performed an evaluation of the impact of water chemistry on foam stability under ambient conditions, employing α-olefin sulfonate surfactant, and different water types, including DI water, seawater, and low-salinity water, were examined. The study concluded that low saline water contributed to greater stability compared with DI water. Additionally, Jiang et al.[15] studied the role of various salt types (NaCl, $CaCl_2$, KCl) and their concentrations on foamability and foam stability. It was observed that foam generation was markedly affected by the type of salt, with foam volume decreasing rapidly upon the addition of $CaCl_2$ and KCl due to interactions between Ca^{2+} and K^+ ions with the SDS surfactant, resulting in crystal formation.

Foam Structure. The structure of foam can be classified into different categories based on the amount of liquid present: dry foam and wet foam. In dry foam, the gas bubbles take on a polyhedral shape with distinct edges, whereas in wet foam, the bubbles are more spherical and stable.[16] However, foam is inherently unstable and has the potential to separate into gas and liquid phases due to its high surface energy.[4] Literature has identified three primary phenomena that contribute to the instability of foam: liquid drainage, coarsening, and bubble coalescence.[17,18] The process of liquid drainage plays a significant role in the degradation of foam, reducing its liquid content, which determines the thickness of the film.[19] This process is driven by gravity and capillary pressure, where the

capillary pressure transfers liquid from the foam film to the plateau borders, while gravity drains the liquid from the network of plateau borders.[20] Bubble coarsening occurs when gas diffuses through the liquid film due to a pressure difference, leading larger bubbles to grow while smaller ones tend to disappear.[21] Bubble coalescence refers to the breaking of adjacent films. To mitigate these phenomena, various chemical additives, primarily surfactants, are employed to enhance foam stability by increasing liquid viscosity and establishing a network of connections between films to minimize liquid drainage and coarsening.[22]

Limited research has delved into the dimensions of bubbles and the mean bubble count during the static test, offering valuable insights into how surfactants, salts, and additives function at the microscopic level to stabilize foam.[23] Foam texture pertains to the dimensions, configurations, and spatial arrangement of bubbles. In general, foam bubbles exhibit diameters ranging from approximately 10 μm to 1 mm.[24] Fine-textured foam refers to instances where bubble sizes are small, while coarse-textured foam describes scenarios with larger bubble sizes.[25] Smaller bubbles, characteristic of fine-textured foam, engender higher viscosity due to a larger interfacial area and augmented film strength, which subsequently results in elevated flow resistance. When the distribution of bubble sizes is narrow and bubbles are uniformly distributed, viscosity tends to be higher.[26]

Foam Drilling Challenges. The challenges posed by the instability of foam in foam drilling are manifold. Foam instability gives rise to a weak structure, high drainage, and low viscosity. In contrast, drilling foams are characterized by their structured nature and high viscosity, which enable them to effectively transport coarse particles.[27] The instability of foam directly impacts the structure of these fluids, resulting in a diminished capacity to carry solids. Moreover, the structural integrity not only affects the foam's lifting capability but also influences its drainage and flow behaviors. Consequently, unstable foams exhibit a lower viscosity compared to their stable counterparts, even when they possess identical compositions. This reduced viscosity, coupled with high drainage, leads to poor hole cleaning and creates various challenges in drilling operations. Stable foams, on the other hand, offer a high level of homogeneity and exhibit consistent and predictable rheological properties. When a flowing foam becomes unstable, it exhibits segregation, the presence of free liquid, and the formation of a two-phase flow. These phenomena cause fluctuations in downhole pressure and temporary overbalance, giving rise to severe formation damage, compromised cleanout performance, and issues with well control.[28,29] Therefore, addressing the challenges associated with unstable foam is crucial for achieving successful foam drilling operations.

When formulating a foam system for use in drilling, the primary consideration is its ability to retain stability under demanding drilling conditions while being compatible with formations sensitive to water. To be deemed an appropriate foam system for underbalanced drilling, specific requirements must be satisfied. These prerequisites encompass the need for adequate stability to facilitate the removal of drill cuttings to the surface, a mild alkaline pH level falling within the range of 9.5 to 10.5 through water treatment, and the ability to withstand the introduction of salts from the formation into the wellbore during underbalanced scenarios, including saline water.[30−32]

To the best of the authors' knowledge, while numerous studies have explored surfactants for foam drilling applications,

there is a noticeable gap in the existing literature regarding the assessment of foam properties such as stability, foamability, bubble characteristics, and structure under alkaline conditions that are of paramount importance in drilling environments. This gap is particularly significant in the context of drilling, where variations in the pressure and temperature play a crucial role. In this study, we utilized an HPHT (high-pressure, high-temperature) foam analyzer to evaluate these foam properties using an eco-friendly foaming agent. Tests were conducted at different pressure levels [14.7 psi (101.35 kPa), 500 psi (3447.37 kPa), and 1000 psi (6894.75 kPa)] and temperatures (25, 50, 75, and 90 °C) in a mildly alkaline environment, mirroring actual field drilling conditions.

Furthermore, this study introduced a unique approach by employing synthesized seawater as the base liquid for the foaming system, which markedly distinguishes it from previous research in the field. Unlike conventional practices that use freshwater for onsite drilling fluid preparation, this innovative step aligns with sustainability and eco-friendly objectives. It delves into the performance of the tested foaming system in a more realistic context, where the liquid base contains a combination of salts, a scenario that differs from the individual salt studies frequently covered in the existing literature. This shift in focus provides a novel perspective on foam stability and behavior.

2. MATERIALS AND METHODS

2.1. Materials. Ammonium alcohol ether sulfate (AAES), an anionic surfactant provided by a service company, was used as

Table 1. Mineral Compositions of Synthesized Seawater

#	Composition	Synthetic sea water (g/L)
1	Na_2SO_4	6.34
2	$NaHCO_3$	0.16
3	$CaCl_2 \cdot 2H_2O$	2.39
4	$MgCl_2 \cdot 6H_2O$	17.64
5	$NaCl$	41.17
Total dissolved solids (TDS), g/L		67.70

the foaming agent in the tested foam systems. AAES has a chemical structure of $[CH_3\text{-}(CH_2)n\text{-}O]_x\text{-}SO_3\text{-}NH_4$, while CH_3 represents a methyl (hydrophobic) group; $(CH_2)_n$ represents a variable-length hydrocarbon chain; SO_3 stands for a sulfonate (hydrophilic) group; and NH_4 represents an ammonium (positively charged) group. It exhibits high biodegradability and has a dual hydrophobic−anionic nature, making it versatile for various applications and enhancing solubility, emulsification, and foaming properties. Nitrogen was selected as the gas phase for the experiments because of its extensive application in foam drilling operations in the field.[33] A synthetic seawater solution with a total salinity of 67.70 g/L and both monovalent and divalent cations was prepared using ACS-grade salts listed in Table 1.[34] To mimic a typical drilling environment, the pH of the foaming solutions was adjusted to a range of 9−10 using a pH buffer solution containing 5 M potassium hydroxide (KOH).

2.2. Sample Preparation. The foaming solutions were prepared by blending 0.5 wt % of the surfactant (AAES) with water using a volumetric flask and a magnetic stirrer. The pH of the solutions was adjusted to the range of 9−10 with the addition of a 5 M KOH solution. To achieve homogeneity, the

solutions were thoroughly mixed for several hours before foaming experiments.

2.3. Testing Devices. *High-Pressure Foam Analyzer (HPFA).* A commercial HPHT foam analyzer (Figure 1) was utilized to assess the foam stability, structure, and bubble size of AAES foam. This sophisticated instrument comprises a high-pressure (HP) view cell for visualizing foam structure and decay, an electric heating jacket for precise temperature control, cameras, transmitted lights, and specialized prisms. It allows the simultaneous measurement of foam height and structure over time through optical methods. Bubble shape and size were analyzed by using high-resolution prisms. The experiment commenced with filling the HP view cell with a surfactant solution followed by heating to the desired temperature. Once the desired temperature was achieved, the solution in the cell was partially drained to a specific level, and then the HP cell view was pressurized with N_2 to reach a pressure of 1000 psi (6894.75 kPa). Foam generation occurred by pumping N_2 from the bottom through a porous plate at a rate of 50 mL/min. A back-pressure regulator was employed to manage increased pressure. Specially installed software facilitated video recording and analysis of the entire foaming and collapsing process, set with a duration of 300 min before automatic termination.

Rheometer. The viscosity of the liquid base is a crucial factor influencing the overall foaming properties in foaming systems.[35] In this research, the viscosity of AAES liquid solutions employed for foam generation was evaluated using an Anton-Paar Rheometer at a shear rate of 600 s^{-1}.

3. RESULTS AND DISCUSSIONS

3.1. Pressure Effect on Foaming. *3.1.1. Testing Conditions.* In this section, AAES foam systems have been experimentally investigated under different pressures [14.7 psi (101.35 kPa), 500 psi (3447.37 kPa), and 1000 psi (6894.75 kPa)] at the same temperature of 50 °C to assess the impact of varying pressures on AAES foam stability, foamability, and bubbles' structure.

3.1.2. Foam Stability. Figure 2 displays the relative volume of AAES foam at different pressures [14.7 psi (101.35 kPa), 500 psi (3447.37 kPa), and 1000 psi (6894.75 kPa)] and a temperature of 50 °C in a mildly alkaline environment (pH ∼ 9.5). The foam decay exhibited variations with pressure, with higher pressures showing reduced foam decay rates, indicating improved foam stability. Figure 3 illustrates the foam half-life, with the AAES foam having the shortest half-life at 14.7 psi (101.35 kPa) (97 min), which more than doubled at 500 psi (3447.37 kPa). Notably, at 1000 psi (6894.75 kPa), the foam stability significantly improved, with only a 20% volume decrease over 350 min, demonstrating highly stable foams. These findings align with prior research, highlighting the positive impact of elevated pressure on foam bubble stability.[36,37]

The observed changes in foam stability with varying pressures can be attributed to the effect of this parameter on the physical properties and behavior of foam. At higher pressures, the gas phase in the foam is compressed, leading to a reduction in the gas volume. This compression of the gas phase helps to stabilize the foam structure by reducing bubble coalescence and promoting stronger bubble films. Consequently, the foam exhibits a slower decay over time, resulting in increased stability. On the other hand, at lower pressures, the gas phase expands, leading to increased bubble coalescence and weaker bubble films, which contribute to faster foam decay and reduced stability.
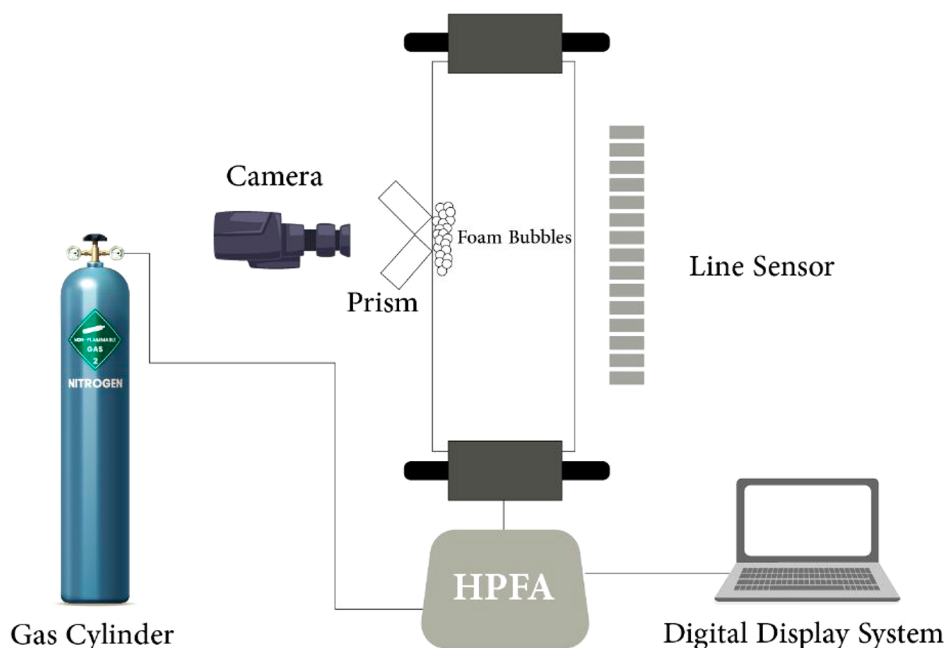
Figure 1. Schematic illustration of the high-pressure foam analyzer HPFA employed for assessing the foam properties.
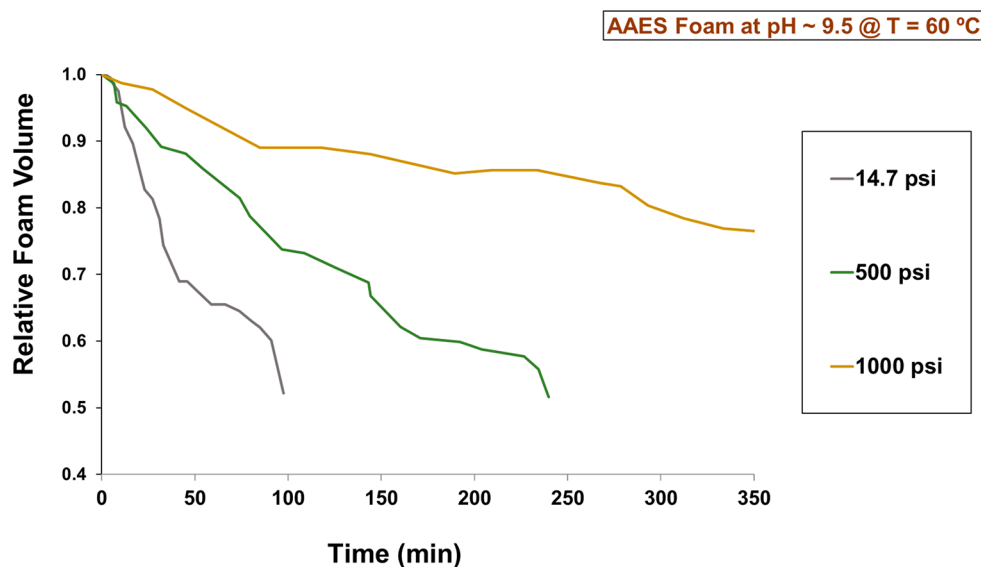

Figure 2. Relative volume of AAES foam under different pressures and at a temperature of 50 °C.

3.1.3. Foamability. Foamability, which assesses a surfactant's inherent capacity to produce foam, is characterized by both the generated foam quantity and the count of gas bubbles (BC) entrapped within the liquid phase. In the foam generation process, nitrogen (N_2) was introduced from the bottom through a porous plate at a consistent flow rate of 50 mL/min until the foam reached its maximum height in the high-pressure (HP) cell view. After gas injection was stopped, the resulting foam underwent evaluation to determine its initial foam volume and the bubble density expressed in bubble count per unit area (bubbles/mm^2). Table 2 presents the average gas volume required to achieve the maximum foam height in each experiment along with the corresponding initial bubble density of the AAES foam.

Increasing the pressure led to a decrease in the amount of gas necessary to attain the maximum foam height in the HP cell.

Specifically, while 149 mL of N_2 gas was needed to generate a full foam column at 14.7 psi (101.35 kPa), this gas volume decreased by 15% at 500 psi (3447.37 kPa) and by 20% at 1000 psi (6894.75 kPa). This phenomenon can be attributed to the rising pressure causing the density of the gas to increase and subsequently reducing surface tension.[37,38] Surface tension is responsible for holding the gas bubbles within the liquid phase and is a critical factor in the foam stability. When the surface tension is lowered, it becomes easier for the gas bubbles to form and stabilize in the liquid, resulting in improved foamability.

Furthermore, the results in Table 2 indicate that the initial bubble density is influenced by the system pressure. Elevating the pressure led to an increase in the initial bubble density observed after stopping the injection of the N_2 gas. At 14.7 psi (101.35 kPa), the AAES foam exhibited the lowest foamability with 35 bubbles per mm^2. However, increasing the pressure to
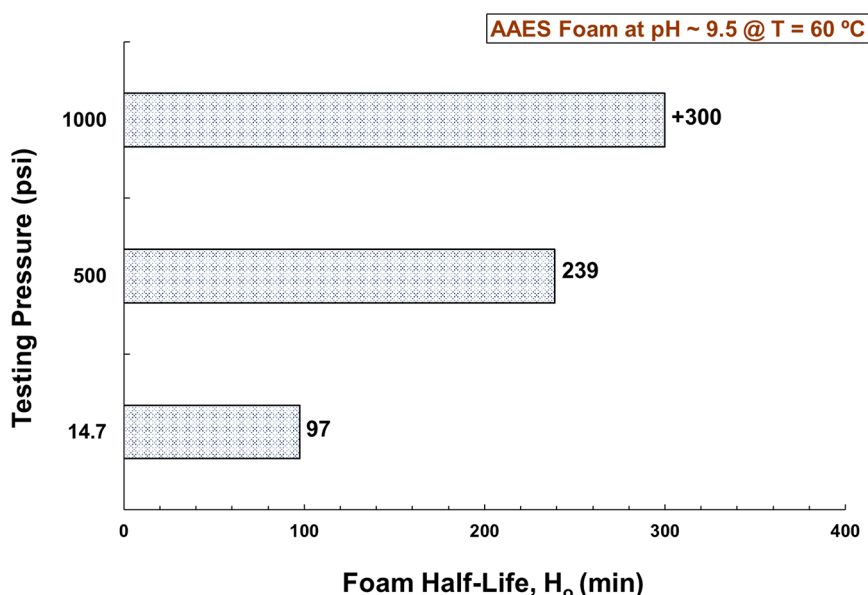
Figure 3. Bubbles' half-life of AAES foam under different pressures and at a temperature of 50 °C.

Table 2. Gas Volume Required to Generate a Full Foam Column under Different Pressures and at Temperature of 50 °C, Expressed in Milliliters (mL), as Well as the Initial Bubble Density

Testing Conditions			
Pressure	Temperature (°C)	Injected N_2 volume (mL)	Initial bubble density (bubbles/mm^2)
14.7 psi (101.35 kPa)	50	149	35
500 psi (3447.37 kPa)		126	51
1000 psi (6894.75 kPa)]		119	80

500 psi (3447.37 kPa) resulted in smaller bubble sizes, leading to a 22% increase in the bubble count per unit area. Further raising the pressure to 1000 psi (6894.75 kPa) enhanced the bubble density to 80 bubbles/mm^2. The reduction in gas volume needed to achieve the maximum foam height at higher pressures suggests that the gas is more efficiently trapped and distributed within the liquid phase.
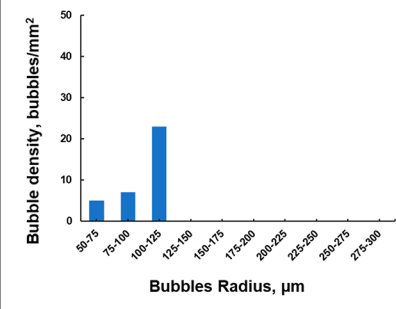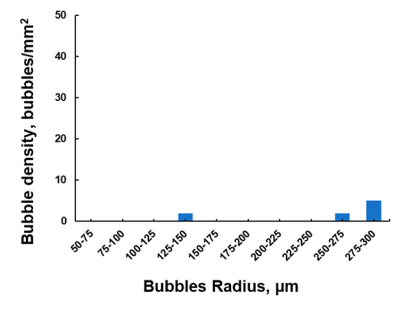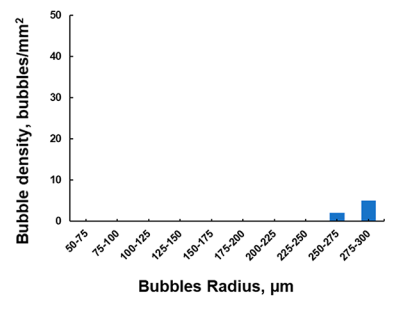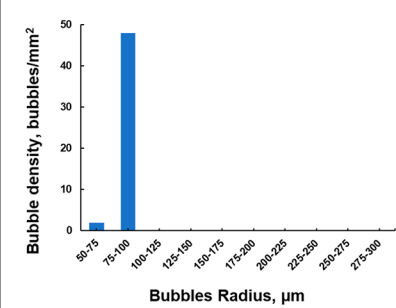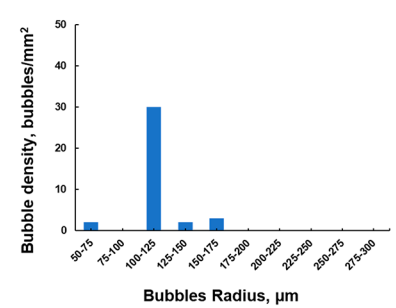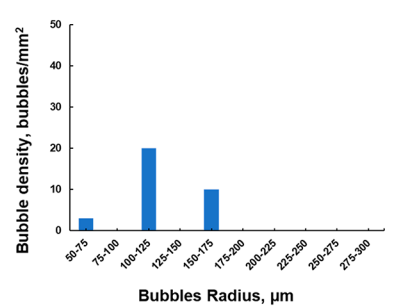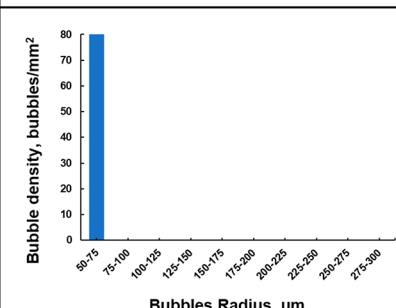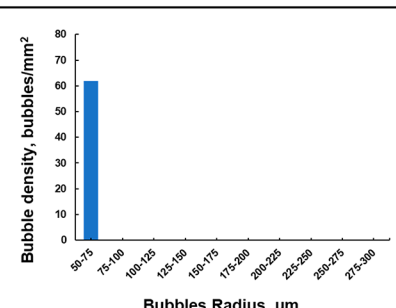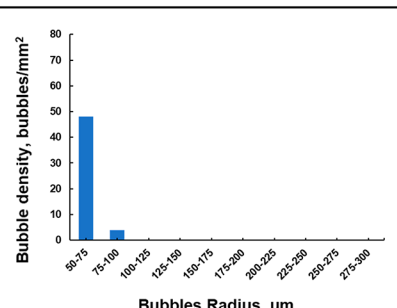
3.1.4. Foam Structure. Table 3 presents the bubble size distributions as a function of time under different pressures and temperature of 50 °C. Images of AAES foam were captured at various time intervals, 1, 30, and 60 min, under different pressures and at a temperature of 50 °C (Table 4). At a pressure of 14.7 psi (101.35 kPa), the analysis revealed the evolution of the foam structure over time. Initially, a nonuniform distribution of bubble sizes was observed, with larger bubbles positioned at the top of the HP cell and smaller ones at the bottom, along with fine-textured bubbles just above the liquid solution. Over time, bubble coarsening occurred as a result of gas diffusion through liquid films due to pressure differences, leading to an increase in bubble size and a reduction in the bubble count per area. After approximately 60 min, a distinct bubble configuration featuring multiple border plateaus was observed at the top of the HP cell. However, when the pressure was increased to 500 psi (3447.37 kPa) and 1000 psi (6894.75 kPa), the bubble size distributions displayed greater uniformity at the beginning of the test, with reduced dominance of bubble coarsening. As time elapsed, numerous small bubbles were observed, indicating the influence of higher pressure on bubble dynamics. The increase in pressure hindered bubble coarsening and enhanced the mechanical strength of the foam structure, preventing bubble merging and

coalescence. Consequently, more small bubbles were retained, resulting in a more uniform bubble size distribution.

The recorded bubble density data in Figure 4 confirmed the observations from the captured images, demonstrating that as time progressed the bubble density decreased with varying rates based on the system pressure. At 14.7 psi (101.35 kPa), a rapid reduction in bubble density to nearly one-third of its initial value was evident, while at 500 psi (3447.37 kPa) and 1000 psi (6894.75 kPa), the rate of bubble count per unit area decrease was notably lower, sustaining a higher bubble count for an extended period. This behavior can be attributed to the pressure's effect on foam stability and bubble coalescence kinetics. At lower pressures, rapid coalescence of gas bubbles led to larger bubbles, thus reducing bubble density. In contrast, at higher pressures, hindered gas diffusion through liquid films resulted in a more uniform distribution of smaller bubbles, contributing to higher bubble density and improved foam stability over time.

Regarding the mean bubble size presented in Figure 5, notable differences are observed primarily at low pressures. Specifically, the initial mean bubble size at 14.7 psi (101.35 kPa) significantly differs from that at higher pressures of 500 psi (3447.37 kPa) and 1000 psi (6894.75 kPa). Over time, the mean bubble size increases at all pressures, with this effect diminishing as the pressure increases, particularly at elevated pressures of 500 psi (3447.37 kPa) and 1000 psi (6894.75 kPa), where the bubble size remains relatively constant. This constancy of bubble size at higher pressures indicates a higher foam stability. The variations in mean bubble size can be attributed to the pressure-dependent bubble coarsening and coalescence kinetics.[37]

Table 3. Histograms of AAES Foam Bubble Distributions at Various Time Intervals under Different Pressures and Temperatures of 50 °C

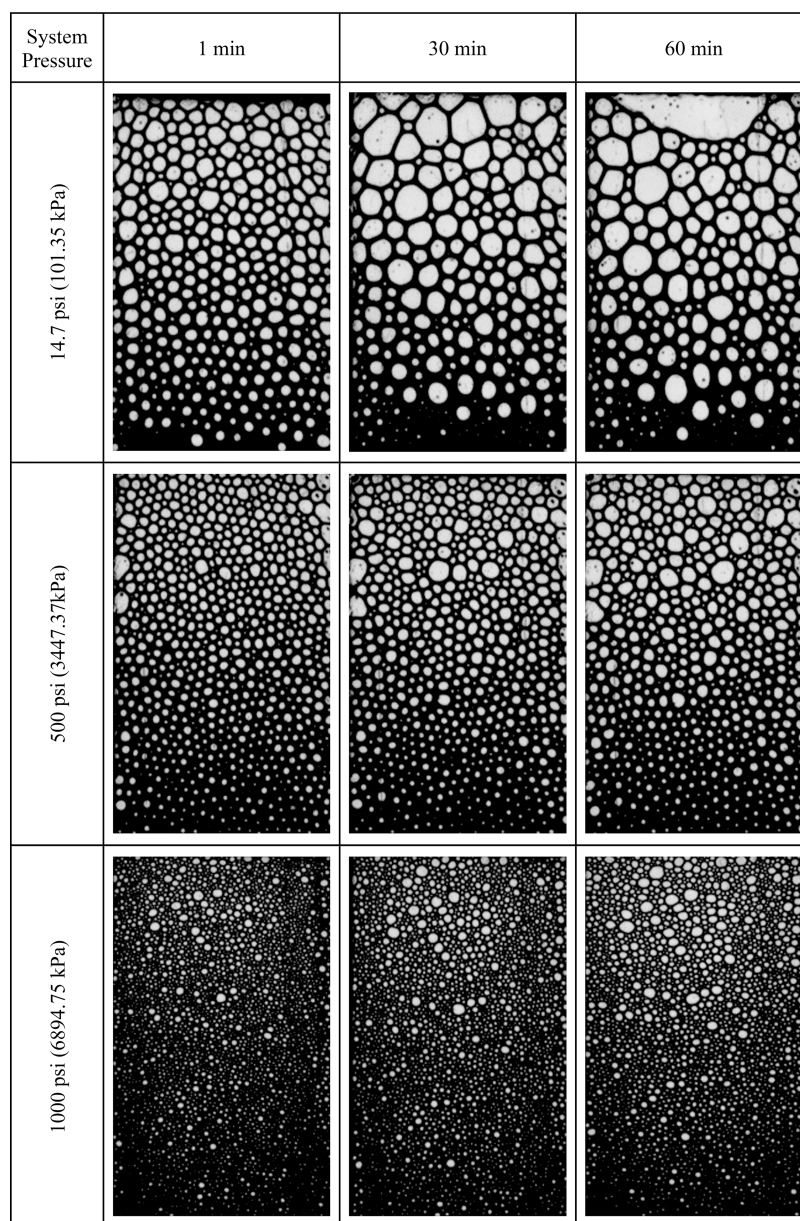| System Pressure.	1 min	30 min	60 min
14.7 psi (101.35 kPa)			
500 psi (3447.37 kPa)			
1000 psi (6894.75 kPa)			

3.2. Temperature Effect on Foaming. *3.2.1. Testing Conditions.* According to the previous section, the findings indicate that pressure positively influences both foam stability and foamability. In light of these results, this section aims to explore AAES foam systems under an elevated pressure of 1000 psi (6894.75 kPa) and varying temperatures (25, 50, 75, and 90 °C) to assess how temperature variations impact AAES foam stability, foamability, and bubble structure.

3.2.2. Foam Stability. Figure 6 illustrates the impact of varying temperatures, along with a pressure of 1000 psi (6894.75 kPa), on the relative volume of AAES foam within a mildly alkaline environment (pH ~ 9.5). The findings indicate a significant influence of temperature on the rate of foam decay, with a notable effect observed at higher temperatures of 75 and 90 °C. Conversely, lower temperatures of 25 and 50 °C exhibited a limited impact on foam decay. These observations can be attributed to the influence of temperature on the kinetics of liquid drainage, coarsening, and bubble coalescence occurring within the foam structure. At higher temperatures of 75 and 90 °C, the increased thermal energy accelerates and enhances the diffusion of gas molecules through liquid films, leading to a more rapid decay of the foam. This results in a notable reduction in the foam's volume over time. Conversely, at lower temperatures of

25 and 50 °C, the reduced thermal energy slows down coarsening and bubble coalescence, leading to a more gradual decay of the foam and thus preserving its volume to a greater extent. These disparities in foam decay rates have direct implications on AAES foam stability, quantified by the half-life of bubbles, as depicted in Figure 7. At temperatures of 50 °C and below, AAES foam demonstrated remarkable stability, with a half-life exceeding 300 min. However, at 75 °C, the foam stability dramatically decreased, showing a half-life of only 60 min, and further reduced to 25 min at 90 °C.

Moreover, an increase in temperature was associated with a clear decrease in the viscosity of the liquid phase, as demonstrated in Figure 7, showing viscosity measurements of the AAES liquid phase under different temperatures and a pressure of 1000 psi (6894.75 kPa). This decrease in liquid viscosity contributes to an accelerated liquid drainage rate from the foam structure, leading to faster foam decay.[39,40] Additionally, the higher temperature increases the surface tension of the foam, which reduces the surface energy of the surfactant molecules.[12] As a result, the surfactant molecules become less effective in maintaining the foam structure, further contributing to the decreased foam stability observed at higher temperatures. Conversely, at lower temperatures of 50 °C and below, the

Table 4. Images of AAES Foam Bubble Structures Were Captured at Various Time Intervals under Different Pressures and Temperatures of 50 °C[a]

System Pressure	1 min	30 min	60 min
14.7 psi (101.35 kPa)			
500 psi (3447.37 kPa)			
1000 psi (6894.75 kPa)			

[a]The foam bubbles are displayed in gray, while the liquid film is represented in black.

reduced rate of liquid drainage, coupled with the higher surface energy of the surfactant molecules, enhances foam stability, leading to an extended half-life of the foam bubbles. The results indicate that the influence of the pressure on AAES foam stability is more pronounced up to 50 °C, but its significance diminishes at higher temperatures (75 and 90 °C). Conversely, the effect of temperature becomes more dominant in determining AAES foam stability at such elevated temperatures.

3.2.3. Foamability. In this subsection, the impact of temperature on the AAES foamability was explored. Table 5 provides the gas volume utilized to attain the maximum foam height in each experimental run along with the associated initial bubble density of the AAES foam. The findings indicate that, under a constant pressure, changes in temperature had a negligible effect on AAES foamability. The gas volume required to achieve the maximum foam height remained nearly consistent

across different temperature conditions. Similarly, the initial bubble density was minimally impacted by temperature variations, with an average of approximately 80 bubbles/mm^2 observed, regardless of the temperature. These results suggest that the initial foamability of AAES is relatively insensitive to temperature changes at such elevated pressure, unlike its foam stability.

3.2.4. Foam Structure. This subsection investigates the influence of temperature variations on the structure of the AAES foam and its evolution over time. Table 6 presents the bubble size distributions as a function of time under different temperatures and pressures of 1000 psi (6894.75 kPa). Table 7 displays images of AAES foam bubble structures captured at different time intervals under various temperatures (25, 50, 75, and 90 °C) and a pressure of 1000 psi (6894.75 kPa). Notably, the foam structure at 25 and 50 °C remains relatively consistent
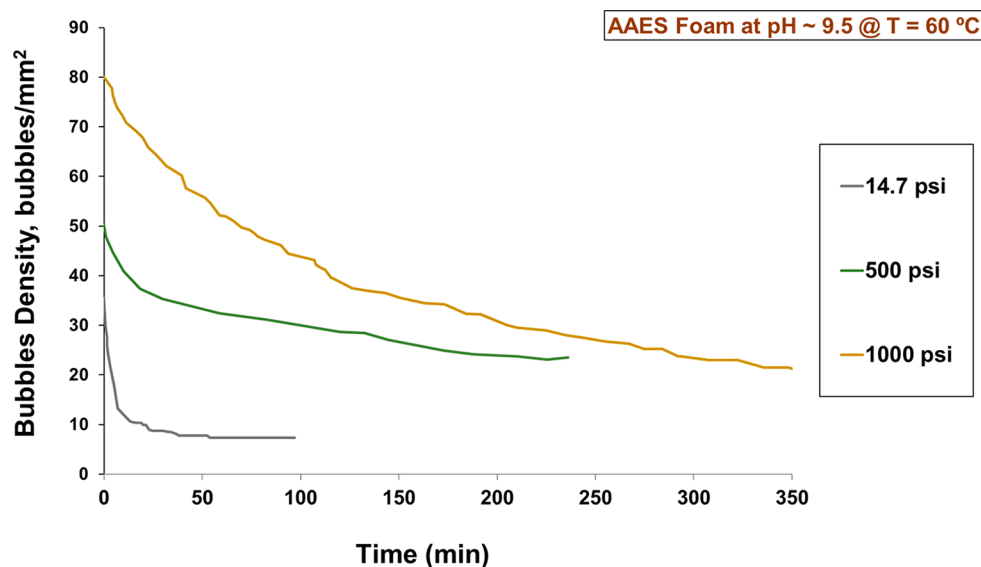
Figure 4. Bubble density as a function of time under different pressures and at a temperature of 50 °C. The graphs display the bubble density up to the half-life of the foam for each experiment.
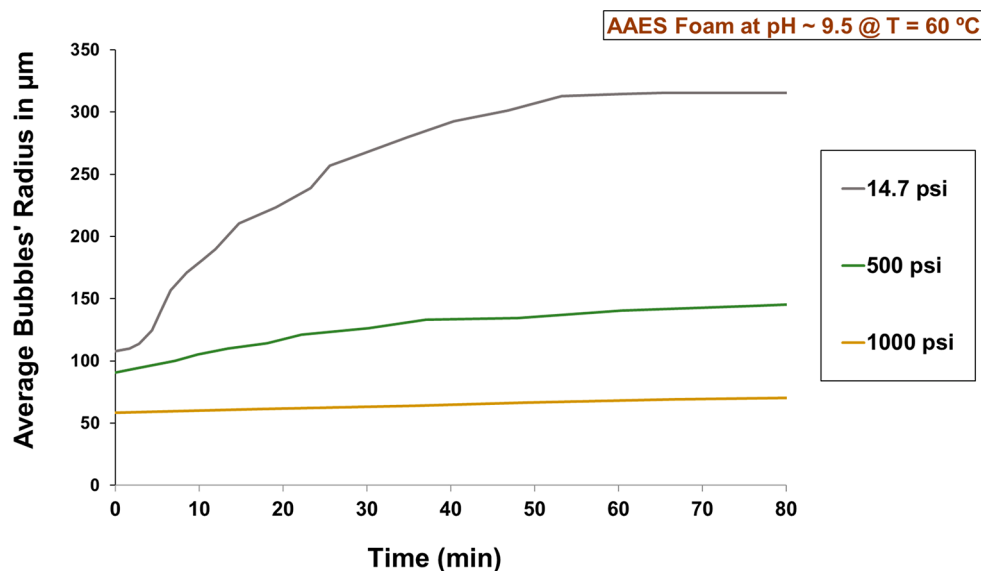

Figure 5. Average bubble radius of AAES foam over time under different pressures and at a temperature of 50 °C.

over time, featuring finely structured and stable foam bubbles. However, at 50 °C, the images reveal a change in foam structure over time, with bubbles enlarging as time progresses. This change in foam structure becomes more significant at 90 °C, where bubbles grow considerably larger after 30 min and mostly diminish after 60 min.

Figure 8 illustrates the average bubble radius of AAES foam over time under different temperatures (25, 50, 75, and 90 °C) and at a pressure of 1000 psi (6894.75 kPa). The bubbles' size remains relatively constant for extended periods at 25 and 50 °C, with an average bubble size of 60 μm. However, the behavior of AAES foam bubbles differs at higher temperatures. At 75 °C, the gradient of the bubble size increase becomes more pronounced, with the mean bubble size increasing by approximately 72% over the foam half-life time of 61 min. The increasing rate of bubble size becomes even more significant at 90 °C, where the average bubble size increases by about 90% in just 25 min. Figure 9 depicts the bubble density over time at different temperatures

and at a pressure of 1000 psi (6894.75 kPa). The graphs illustrate the bubble density up to the foam's half-life for each experiment. The observations in Figure 9 align with the earlier findings and reveal that the number of bubbles per unit area decreases at higher rates with an increasing temperature. These results shed light on the intricate relationship between temperature and AAES foam structure and behavior. The remarkable stability and consistency of foam at lower temperatures suggests its promising potential applicability at surface and intermediate drilling sections. However, at higher temperatures, changes in foam structure and bubble size were evident, highlighting the need for a comprehensive understanding of these dynamics to optimize the performance of AAES foam at elevated temperatures and deeper sections. The efficiency of AAES foam can be further enhanced by incorporating additional additives that offer prolonged stability to the foam structure under such challenging conditions.
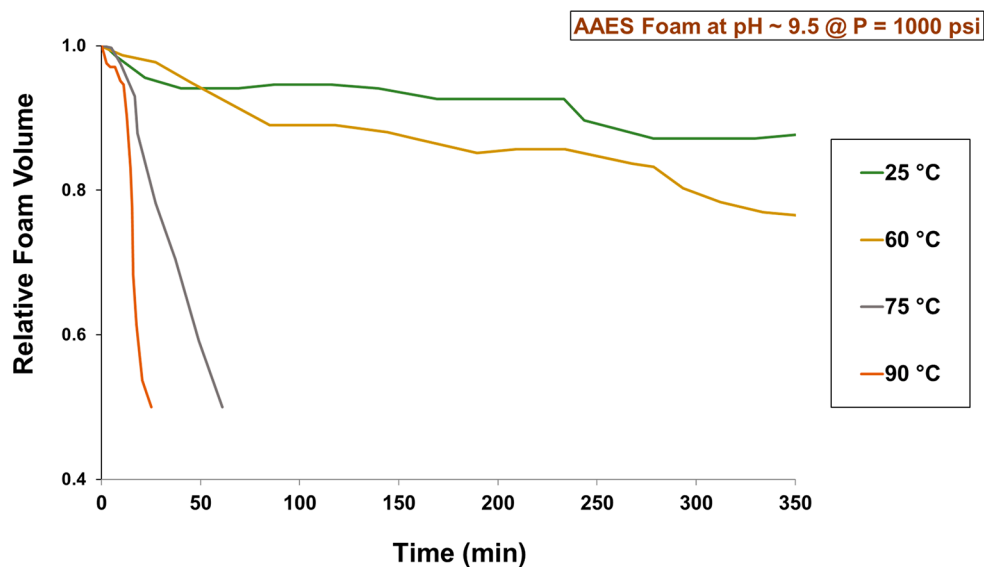
Figure 6. Relative foam volume over time of AAES foam under different temperatures and at a pressure of 1000 psi (6894.75 kPa).
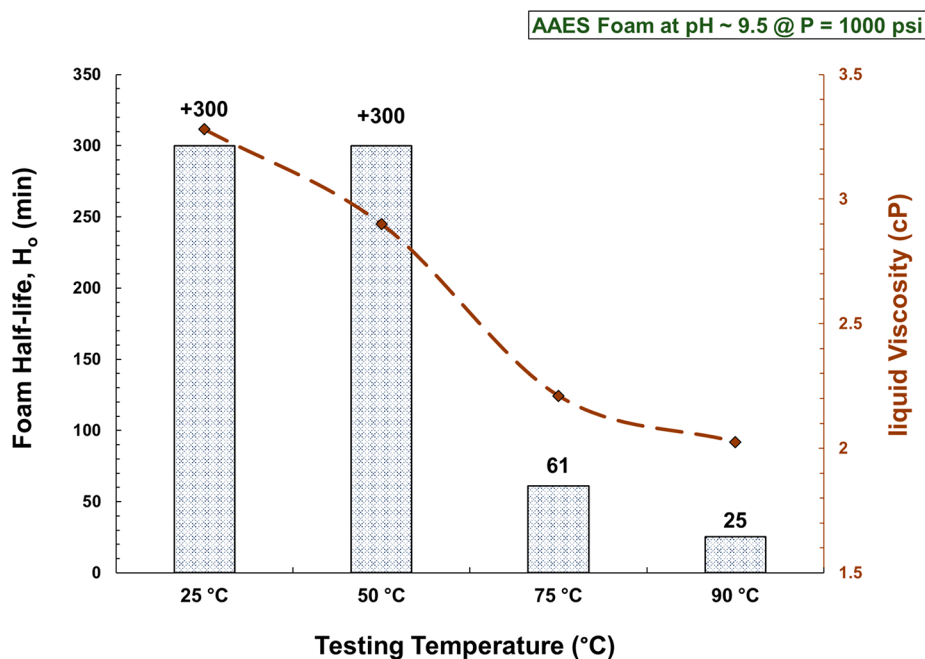

Figure 7. Bubbles' half-life of AAES foam as well as the viscosity measurements of the AAES liquid phase at a shear rate of 600 s^{-1} under different temperatures and at a pressure of 1000 psi (6894.75 kPa).

Table 5. Gas Volume Required to Generate a Full Foam Column under Different Temperatures and at a Pressure of 1000 psi (6894.75 kPa), Expressed in Milliliters (mL), as Well as the Initial Bubble Density Measured in bubbles/mm^{-2}

Pressure	Testing Conditions		
	Temperature (°C)	Injected N$_2$ volume (mL)	Initial bubble density (bubbles/mm^2)
1000 psi (6894.75 kPa)	25	130	76
	50	126	80
	75	122	82
	90	133	74

4. CONCLUSIONS

In this study, the effects of pressure and temperature on AAES foam stability were explored in a simulated mildly alkaline drilling environment by using an advanced high-pressure foam analyzer. To promote sustainability, we substituted freshwater with seawater, which is a more abundant resource. The key findings can be summarized as follows:

- Foam decay rates varied with pressure, showing enhanced stability at higher pressures.

Table 6. Histograms of AAES Foam Bubble Distributions at Various Time Intervals under Different Temperatures and a Pressure of 1000 psi (6894.75 kPa)

| System Temp.	1 min	30 min	60 min
25 °C			
50 °C			
75 °C			
90 °C			

- Increasing pressure reduced the gas volume needed for maximum foam height and increased initial bubble density.
- Under 14.7 psi (101.35 kPa), foam structure evolved over time with nonuniform bubble size distribution. At 500 (3447.37 kPa) and 1000 psi (6894.75 kPa), foam exhibited greater uniformity with smaller bubbles.
- Temperature significantly affected foam decay, especially at 75 and 90 °C, due to decreased liquid viscosity, accelerating foam decay by faster liquid drainage.
- Pressure's impact on AAES foam stability was more pronounced at temperatures up to 50 °C, diminishing at

higher temperatures (75 and 90 °C). Conversely, temperature became dominant in determining foam stability at elevated temperatures.

- Under constant pressure, temperature had a minimal impact on AAES foamability, maintaining consistent gas volume for maximum foam height. However, foam stability proved more sensitive to temperature changes, with a notable increase in bubble size gradient.

These findings highlight AAES foam's suitability for surface and intermediate drilling in lower-temperature environments while emphasizing the need to understand foam dynamics at

Table 7. Images of AAES Foam Bubble Structures Were Captured at Various Time Intervals under Different Temperatures and a Pressure of 1000 psi (6894.75 kPa)[a]

System Temp.	1 min	30 min	60 min
25 °C			
50 °C			
75 °C			
90 °C			
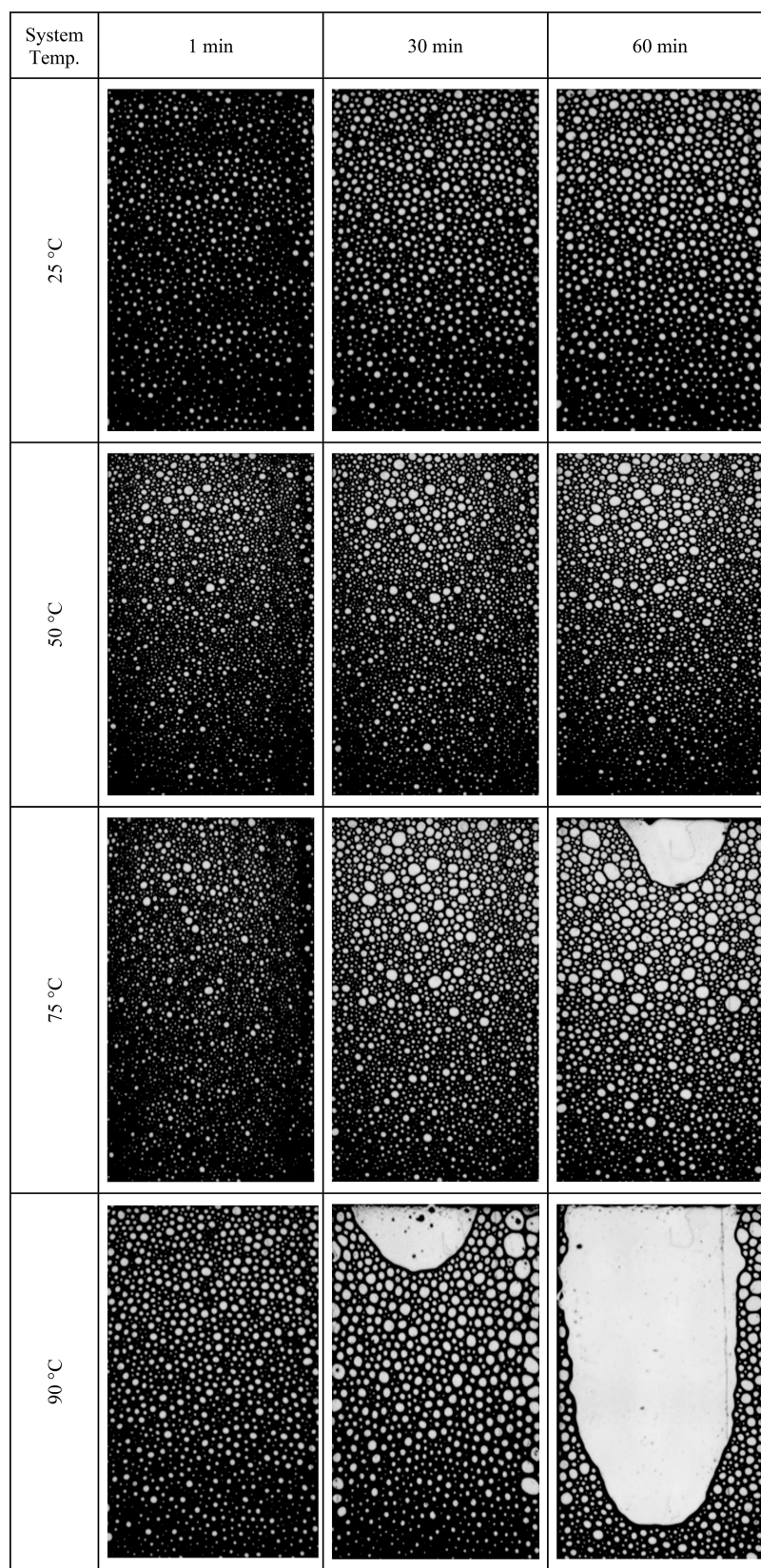
[a]The foam bubbles are displayed in grey, while the liquid film is represented in black.

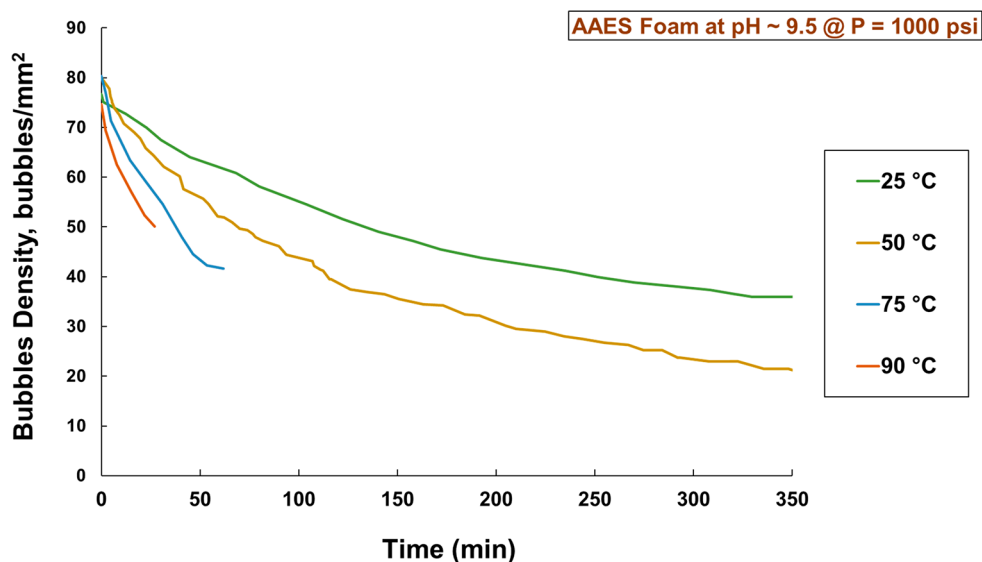higher temperatures and greater depths for optimized drilling performance.

Figure 8. Average bubbles' radius of AAES foam over time under different temperatures and at a pressure of 1000 psi (6894.75 kPa).
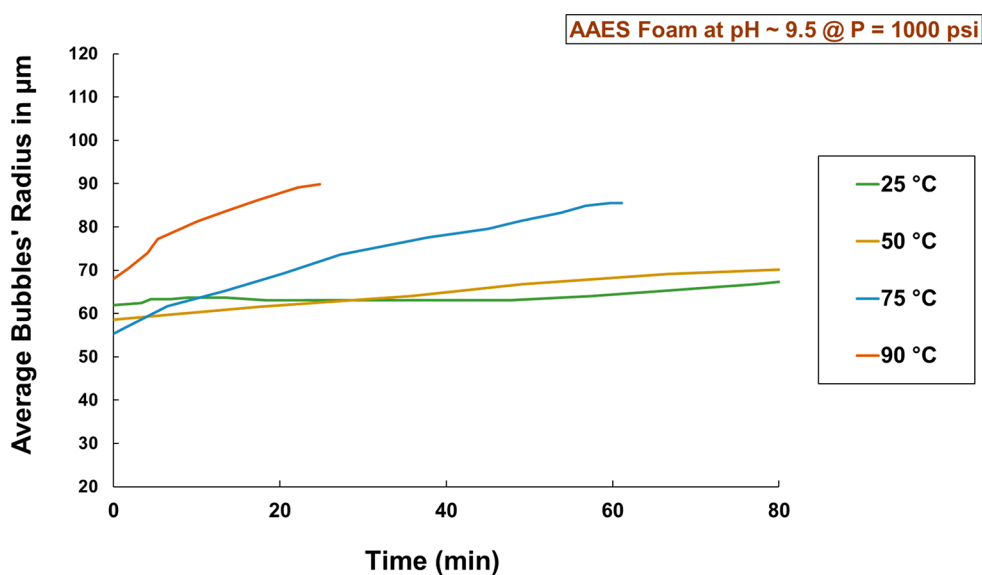

Figure 9. Bubble density as a function of time under different temperatures and a pressure of 1000 psi (6894.75 kPa). The graphs display the bubble density up to the half-life of the foam for each experiment.

■ AUTHOR INFORMATION

Corresponding Author

Salaheldin Elkatatny — *College of Petroleum Engineering and Geosciences, King Fahd University of Petroleum & Minerals, 31261 Dhahran, Saudi Arabia;* ● orcid.org/0000-0002-7209-3715; Phone: +966-594663692; Email: elkatatny@kfupm.edu.sa

Authors

Ahmed Gowida — *College of Petroleum Engineering and Geosciences, King Fahd University of Petroleum & Minerals, 31261 Dhahran, Saudi Arabia*

Ahmed Farid Ibrahim — *College of Petroleum Engineering and Geosciences, King Fahd University of Petroleum & Minerals, 31261 Dhahran, Saudi Arabia;* ● orcid.org/0000-0001-7258-8542

Muhammad Shahzad Kamal — *Center for Integrative Petroleum Research, King Fahd University of Petroleum & Minerals, 31261 Dhahran, Saudi Arabia;* ● orcid.org/0000-0003-2359-836X

Author Contributions

Conceptualization, S.E. and A.G.; methodology, M.S., A.G., and A.I.; formal analysis, A.G.; investigation, A.G. and A.I.; data curation, A.G.; writing—original draft preparation, A.G. and S.E.; writing—review and editing, M.S., A.I., and S.E.; supervision, SE. All authors have read and agreed to the published version of the manuscript.

Notes

The authors declare no competing financial interest.

■ NOMENCLATURE

AAES, Ammonium alcohol ether sulfate; $BC_{Initial}$, Initial bubble count; DI, Deionized water; Ho, Foam half lifetime; RFV, Relative foam volume; SDS, Sodium dodecyl sulfate; UBD, Underbalanced drilling; $V_{Initial}$, Initial Foam Volume

■ REFERENCES

(1) Ojha, K.; Saxena, A.; Pathak, A. K. Underbalanced Drilling and Its Advancements: An Overview. *Journal of Petroleum Engineering and Technology* **2014**, *4* (2).

(2) Lioumbas, J. S.; Georgiou, E.; Kostoglou, M.; Karapantsios, T. D. Foam Free Drainage and Bubbles Size for Surfactant Concentrations below the CMC. *Colloids Surf., A* **2015**, *487*, 92−103.

(3) Ramadan, A.; Kuru, E.; Saasen, A. Critcal Review of Drilling Foam Rheology. *Annual Transactions-Nordic Rheology Society* **2003**, *11*, 63−72.

(4) Wang, J.; Nguyen, A. V.; Farrokhpay, S. A Critical Review of the Growth, Drainage and Collapse of Foams. *Adv. Colloid Interface Sci.* **2016**, *228*, 55−70.

(5) Obisesan, O.; Ahmed, R.; Amani, M. The Effect of Salt on Stability of Aqueous Foams. *Energies* **2021**, *14* (2), 279.

(6) Memon, M. K.; Elraies, K. A.; Al-Mossawy, M. I. A. Surfactant Screening to Generate Strong Foam with Formation Water and Crude Oil. *Journal of Petroleum Exploration and Production Technology* **2021**, *11*, 3521−3532.

(7) Bashir, A.; Sharifi Haddad, A.; Rafati, R. An Experimental Investigation of Dynamic Viscosity of Foam at Different Temperatures. *Chem. Eng. Sci.* **2022**, *248*, 117262.

(8) Ibrahim, A. F.; Nasr-El-Din, H. A. CO 2 Foam for Enhanced Oil Recovery Applications. In *Foams-Emerging Technologies*; IntechOpen, 2019.

(9) Wang, Y.; Zhang, Y.; Liu, Y.; Zhang, L.; Ren, S.; Lu, J.; Wang, X.; Fan, N. The Stability Study of CO2 Foams at High Pressure and High Temperature. *J. Pet. Sci. Eng.* **2017**, *154*, 234−243.

(10) Al-Darweesh, J.; Aljawad, M. S.; Al-Yousif, Z.; BinGhanim, A.; Kamal, M. S.; Mahmoud, M. The Impact of Green Chelating Agent and Corrosion Inhibitor on Foam Rheology and Stability at High Temperature, Pressure, and Salinity. *SPE Journal* **2023**, *28* (03), 1216−1229.

(11) Al-Darweesh, J.; Aljawad, M. S.; Al-Ramadan, M.; Elkatatny, S.; Mahmoud, M.; Patil, S. Review of Underbalanced Drilling Techniques Highlighting the Advancement of Foamed Drilling Fluids. *Journal of Petroleum Exploration and Production Technology* **2023**, *13* (4), 929−958.

(12) Guo, Y. On the Stability of Aqueous Foams and the Effect of Surfactant. *Master's thesis*, University of Calgary, Calgary, Canada, 2021. https://prism.ucalgary.ca; https://hdl.handle.net/1880/113820.

(13) Majeed, T.; Sølling, T. I.; Kamal, M. S. Foamstability: The Interplay between Salt-, Surfactant-and Critical Micelle Concentration. *J. Pet. Sci. Eng.* **2020**, *187*, 106871.

(14) AlYousef, Z.; Ayirala, S.; Gizzatov, A.; Kokal, S. Evaluating Foam Stability Using Tailored Water Chemistry for Gas Mobility Control Applications. *J. Pet. Sci. Eng.* **2020**, *195*, 107532.

(15) Jiang, N.; Yu, X.; Sheng, Y.; Zong, R.; Li, C.; Lu, S. Role of Salts in Performance of Foam Stabilized with Sodium Dodecyl Sulfate. *Chem. Eng. Sci.* **2020**, *216*, 115474.

(16) Isabelle, C.; Sylvie, C. A.; Florence, E.; François, G.; Reinhard, H.; Olivier, P.; Florence, R.; Arnaud, S. J.; Ruth, F. *Foams: Structure and Dynamics*; Oxford Univ. Press, 203AD.

(17) Koehler, S. A.; Hilgenfeldt, S.; Stone, H. A. A Generalized View of Foam Drainage: Experiment and Theory. *Langmuir* **2000**, *16* (15), 6327−6341.

(18) Pitois, O.; Fritz, C.; Vignes-Adler, M. Liquid Drainage through Aqueous Foam: Study of the Flow on the Bubble Scale. *J. Colloid Interface Sci.* **2005**, *282* (2), 458−465.

(19) Kruglyakov, P. M.; Karakashev, S. I.; Nguyen, A. V.; Vilkova, N. G. Foam Drainage. *Curr. Opin. Colloid Interface Sci.* **2008**, *13* (3), 163−170.

(20) Lioumbas, J. S.; Georgiou, E.; Kostoglou, M.; Karapantsios, T. D. Foam Free Drainage and Bubbles Size for Surfactant Concentrations below the CMC. *Colloids Surf., A* **2015**, *487*, 92−103.

(21) Zhou, J.; Ranjith, P. G.; Wanniarachchi, W. A. M. Different Strategies of Foam Stabilization in the Use of Foam as a Fracturing Fluid. *Adv. Colloid Interface Sci.* **2020**, *276*, 102104.

(22) Angarska, J.; Stubenrauch, C.; Manev, E. Drainage of Foam Films Stabilized with Mixtures of Non-Ionic Surfactants. *Colloids Surf., A* **2007**, *309* (1), 189−197.

(23) Al-Darweesh, J.; Aljawad, M. S.; Kamal, M. S.; Mahmoud, M.; Al-Yousef, Z.; Al-Shehri, D. Water Chemistry Role in the Stability of CO2 Foam for Carbon Sequestration in Water Aquifers. *Gas Science and Engineering* **2023**, *118*, 205090.

(24) Den Engelsen, C. W.; Isarin, J. C.; Gooijer, H.; Warmoeskerken, M.; Wassink, J. G. Bubble Size Distribution of Foam. *Autex Res. J.* **2002**, *2* (1), 14.

(25) Eren, T. *Foam Characterization: Bubble Size and Texture Effects*; Middle East Technical University, 2004. DOI: DOI: 10.13140/RG.2.2.24491.69920.

(26) Harris, P. C. Effects of Texture on Rheology of Foam Fracturing Fluids. *SPE production engineering* **1989**, *4* (03), 249−257.

(27) Govindu, A.; Ahmed, R.; Shah, S.; Amani, M. The Effect of Inclination on the Stability of Foam Systems in Drilling and Well Operations. *SPE Drilling & Completion* **2021**, *36* (02), 263−280.

(28) Herzhaft, B.; Toure, A.; Bruni, F.; Saintpere, S. Aqueous Foams for Underbalanced Drilling: The Question of Solids. In *SPE Annual Technical Conference and Exhibition*; OnePetro, 2000.

(29) Ding, Y.; Herzhaft, B.; Renard, G. Near-Wellbore Formation Damage Effects on Well Performance: A Comparison between Underbalanced and Overbalanced Drilling. *SPE Production & Operations* **2006**, *21* (01), 51−57.

(30) IADC UBD Committee. *IADC Well Classification System for Underbalanced Operations and Managed Pressure Drilling*; Adopted by the IADC Board of Directors, 2005.

(31) API-RP-92U. *Underbalanced Drilling Operations, API Recommended Practice 92U*; American Petroleum Institute Washington, 2008.

(32) Sepulveda, J. J.; Falana, O. M.; Kakadjian, S.; Morales, J. D.; Zamora, F.; DiBiasio, M.; Marshall, E. C.; Shirley, G. L.; Benoit, D. J.; Tkach, S. A. Oil-Based Foam and Proper Underbalanced-Drilling Practices Improve Drilling Efficiency in a Deep Gulf Coast Well. In *SPE Annual Technical Conference and Exhibition*; OnePetro, 2008.

(33) Rehm, B.; Haghshenas, A.; Paknejad, A. S.; Al-Yami, A.; Hughes, J. *Underbalanced Drilling: Limits and Extremes*; Elsevier, 2013.

(34) Al-Darweesh, J.; Aljawad, M. S.; Al-Yousef, Z.; BinGhanim, A.; Kamal, M. S.; Mahmoud, M. Corrosion Inhibitor and Chelating Agent Impact on Foam Stability for Formation Stimulation Applications. *Geoenergy Science and Engineering* **2023**, *222*, 211434.

(35) Brown, A. G.; Thuman, W. C.; McBain, J. W. The Surface Viscosity of Detergent Solutions as a Factor in Foam Stability. *Journal of Colloid Science* **1953**, *8* (5), 491−507.

(36) Pradhan, M. S.; Khilar, K. C. Stability of Aqueous Foams with Polymer Additives: III. Measurements and Calculations of Stability of Foams Generated at Different Pressures. *J. Colloid Interface Sci.* **1994**, *168* (2), 333−338.

(37) Szabries, M.; Sergelius, S.; Kordts, A.; Jönsson, M. Foam Stability and Foam Structure under High Pressure for Tertiary Oil Production. *Appl. Rep* **2019**, 1−5.

(38) Al-Darweesh, J.; Aljawad, M. S.; AlYousef, Z.; BinGhanim, A.; Kamal, M. S.; Mahmoud, M.; Al-Shehri, D. Investigation of Amine-Based Surfactants for Foamed Acid Stimulation at High Temperature, Pressure, and Salinity. *Geoenergy Science and Engineering* **2023**, *229*, 212094.

(39) Kapetas, L.; Bonnieu, S. V.; Danelis, S.; Rossen, W. R.; Farajzadeh, R.; Eftekhari, A. A.; Shafian, S. R.; Bahrim, R. Z. Effect of Temperature on Foam Flow in Porous Media. In *SPE Middle East Oil & Gas Show and Conference*; OnePetro, 2015.

(40) Kamal, M. S. A Novel Approach to Stabilize Foam Using Fluorinated Surfactants. *Energies* **2019**, *12* (6), 1163.